Polymer Chemistry

Accepted Manuscript

ROYAL SOCIETY OF CHEMISTRY

www.rsc.org/polymers

Journal Name

RSCPublishing

ARTICLE

Side chain effect on difluoro-substituted dibenzo[a,c]phenazine based conjugated polymers as donor materials for high efficiency polymer solar cells

Cite this: DOI: 10.1039/x0xx00000x

Received 00th January 2012,
Accepted 00th January 2012

DOI: 10.1039/x0xx00000x

www.rsc.org/

Guangwu Li,[1] Zhen Lu,[1] Cuihong Li,[*,1] Zhishan Bo[*,1]

Two conjugated polymers with benzodithiophene derivatives as the donor unit and planar difluoro-substituted dibenzo[a,c]phenazine as the acceptor unit **P1**, **P2-L** and **P2-H** were designed, synthesized, and used as the donor material used in the polymer solar cells. **P2-H** exhibit the highest hole mobility with 1.54×10^{-2} $cm^2V^{-1}s^{-1}$. Polymer solar cells (PSCs) with the blend of **P1**:$PC_{71}BM$ (1:1.5, by weight) as the active layer show the highest power conversion efficiency (PCE) of 6.0% in those polymers with an open circuit voltage (V_{oc}) of 0.74 V, a short circuit current (J_{sc}) of 12.50 mA/cm^2, and a fill factor (*FF*) of 0.65.

Introduction

The characteristics of polymer solar cell (PSC) such as light weight, flexible, and being able to be produced by low cost inkjet printing and roll-to-roll processes have made PSC an unique member of solar cell family.[1-3] Intensive researches on designing new material,[4-7] device innovation,[8-10] and interfacial modification[11-14] in the last decade have rapidly enhanced the power conversion efficiency of PSCs up to 11%.[15] The intrinsic properties of conjugated polymers have a great influence on the performances of PSCs, and the creation of new polymer donor materials has done a great contribution to the rapid development of PSCs.[4,16-19] Researches on developing new materials are mainly focused on the synthesis of new donor-acceptor (D-A) type small band gap polymers that can harvest more sun light to generate higher short-circuit current density (J_{sc}).[20]

Quinoxaline derivatives with two electron-withdrawing imine nitrogen atoms have been widely used as the acceptor units for the synthesis of D–A polymers and their power conversion efficiency (PCE) has reached more than 8%.[21-24] The solubility and electronic properties of quinoxaline derivatives can be tuned by the variation of the substituents.[25-28] D-A polymers with planar quinoxaline acceptor unit exhibit much better photovoltaic performance than the corresponding less planar quinoxaline acceptor unit.[29-32] Dibenzo[a,c]phenazine has been used to construct many D-A alternating conjugated polymers.[33-36] In addition, the introduction of fluoro substituents on the acceptor units has been demonstrated to be a very efficient strategy to improve PCE of PSCs, fluorine substituents can lower the HOMO and LUMO energy levels of resulted conjugated polymers to afford higher open circuit voltage (V_{oc}), increase the intramolecular polymer chain interaction to have higher hole mobility, and reduce the charge recombination to achieve higher efficiency.[37-40] Here, we designed and synthesized two D-A alternating conjugated polymers **P1** and **P2** with a planar polyaromatic quinoxaline derivative, 11,12-difluorodibenzo[a,c]phenazine, as the acceptor unit and benzodithiophene derivatives as the donor unit. The influences of side chains at the benzodithiophene unit and the molecular weight of polymers on the photovoltaic performance of PSCs were investigated. **P2-H** exhibit the highest hole mobility with 1.54×10^{-2} $cm^2V^{-1}s^{-1}$. Polymer solar cells (PSCs) with the blend of **P1**:$PC_{71}BM$ (1:1.5, by weight) as the active layer show the highest PCE of 6.0% in these polymers with an open circuit voltage (V_{oc}) of 0.74 V, a short circuit current density (J_{sc}) of 12.50 mA/cm^2, and a fill factor (*FF*) of 0.65.

RESULTS AND DISCUSSION

Material Synthesis and Characterization

The syntheses of monomers and polymers are outlined in Scheme 1. Compound **1** was synthesized according to the literature procedures.[41] The reduction of compound **1** with zinc dust in hot acetic acid afforded the corresponding diamine, which was used for next step without further purification. The condensation of the diamine with phenanthrene-9,10-dione afforded compound **2** in a total yield of 61%. Bromination of

compound **2** with Br_2 in CH_2Cl_2 afforded **M1** in a yield of 91%. The polymerization of **M1** with **M2** and **M3** afforded **P1** and **P2,** respectively. **P2** was fractioned into low molecular weight fraction (**P2-L**) and high molecular weight fraction (**P2-H**) according to their solubility in chloroform. **P2-L** can be dissolved in hot chloroform. **P1** and **P2-H** exhibited limited solubility in common chlorinated organic solvents such as CB, DCB, and TCB at room temperature, but can be fully dissolved

Scheme 1. Synthetic route of **P1** and **P2**

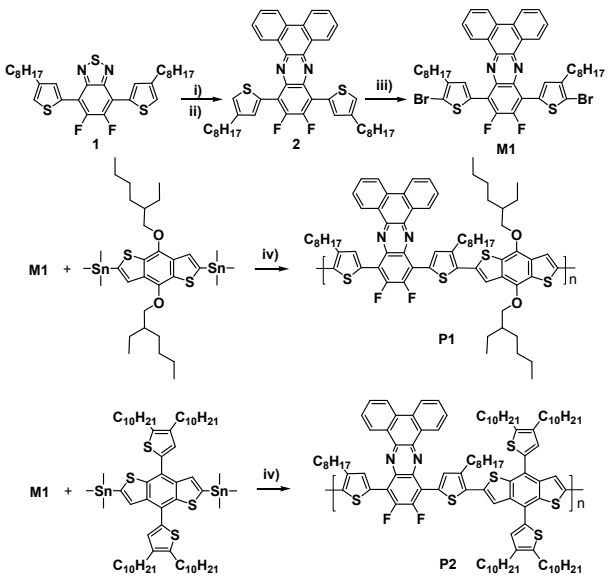

i) Zn, AcOH; ii) phenanthrene-9,10-dione, 80 °C; iii) NBS, $CHCl_3$, rt; vi) toluene/DMF (v:v,10:1), $Pd(PPh_3)_4$, reflux.

in these solvents at elevated temperature. Molecular weights and their distributions were measured by gel permeation chromatography (GPC) using TCB as an eluent at 150 °C with narrowly distributed polystyrenes as the calibration standards, and the results are summarized in Table 1. These three polymers are of good thermal stability as indicated by thermo gravimetric analysis (TGA) measurements. The 5% decomposition temperatures of **P1**, **P2-L**, and **P2-H** are also shown in Table 1. Differential scanning calorimetry (DSC) measurements from 20 to 300 °C under nitrogen atmosphere showed that there is no obvious glass transition for these polymers. Powdery X-ray diffraction (XRD) measurements were carried out to investigate the packing of polymer chains in solid state. As shown in Figure 1, XRD diffraction patterns of **P1** exhibited two diffraction peaks. The first peak at small angle region, which reflexes the distance of polymer backbones separated by the flexible side chains, is located at 2θ of 5.14 °, corresponding to a distance of 17.2 Å.[42] The second peak at the wide angle region reflex the π-π stacking distances between polymer backbones, which is located at 2θ of 22.6 °, corresponding to a distance of 3.9 Å.[42] **P2-L** and **P2-H** exhibit only a broad peak in the wide angle region, which is located at 20.9 °, corresponding to a distance of 4.3 Å. For **P2**, the lack of diffraction peak in small angle region indicated that **P2** formed a less ordered packing in solid state as compared with **P1**. Compared with **P1**, the larger π-π stacking distance of **P2** in the solid state reflexes that the two 4,5-didecylthienyl substituents at the 4,8-position of benzodithiophene can prevent the close and ordered packing of polymer chains in the solid state. The results are consistent with the photovoltaic device results.

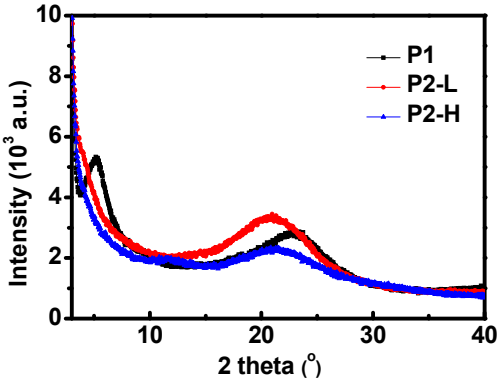

Fig. 1 XRD curves of polymers powdery samples.

Table 1. Physical Properties of the polymers

polymer	M_n (kg/mol)[a]	M_w (kg/mol)[a]	D	T_d (°C)[b]
P1	28.0	59.9	2.38	318
P2-L	34.7	72.6	2.09	427
P2-H	63.7	113.2	1.77	439

[a] M_n, M_w, and dispersity (D) of polymers were determined by GPC at 150 °C using polystyrene standards with TCB as an eluent. [b] Decomposition temperatures were determined by TGA under N_2 based on 5% weight loss.

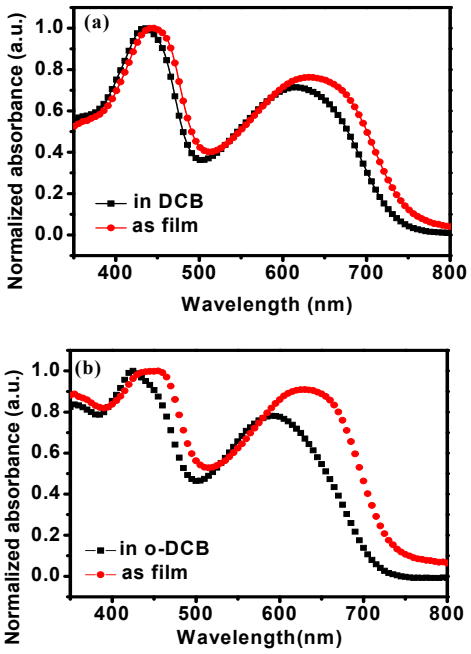

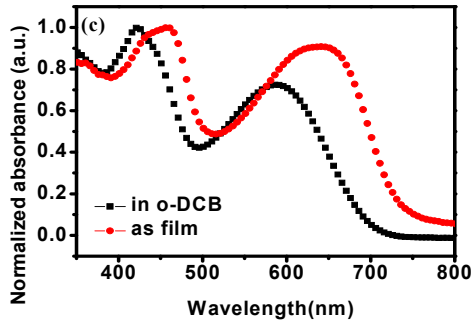

Fig. 2 UV-vis absorption spectra of (a) **P1**, (b) **P2-L**, and (c) **P2-H** in DCB solutions and as thin films

Electrochemical Properties. Electrochemical properties of **P1**, **P2-L**, and **P2-H** were investigated by cyclic voltammetry (CV) using a standard three electrodes electrochemical cell. As shown in Figure 3, these three polymers exhibited irreversible redox processes. The onset oxidation potentials of **P1**, **P2-L**, and **P2-H** are 0.59, 0.80, and0.80 V, respectively. HOMO levels of **P1**, **P2-L**, and **P2-H** were determined, using the equation E_{HOMO} = -e(E_{ox} + 4.71), to be -5.30, -5.51, and -5.51 eV, respectively. LUMO levels of **P1**, **P2-L**, and **P2-H** were therefore calculated according to the equation E_{LUMO} = E_{HOMO} + $E_{g,opt}$ to be -3.64, -3.81, and -3.81 eV, respectively. The data are also summarized in Table 2.

Table 2. Electrochemical and optical properties of polymers**.**

polymer	λ_{max} [nm] solution [a]	λ_{max} [nm] film	λ_{edge} [nm]	$E_{g,opt}$ (eV)[b]	HOMO (eV)	LUMO (eV)[c]
P1	431, 614	442, 631	746	1.66	-5.30	-3.64
P2[d]	421, 591	453, 631	729	1.70	-5.51	-3.81

[a] measured at 100 °C. [b] calculated from the absorption band edge of the copolymer film, $E_{g,opt}$ = 1240/$\lambda_{edge.}$ [c] calculated by the equation E_{LUMO} = E_{HOMO} + $E_{g,opt}$. [d]**P2-L** and **P2-H** have the same optical properties.

Optical Properties. Optical properties of **P1** and **P2** in solutions and as thin films are investigated by UV-visible absorption spectroscopy and shown in Figure 2. The optical properties of low and high molecular weight polymer **P2** are exactly the same, so here we did not differentiate **P2-L** and **P2-H**. UV-vis absorption spectra of **P1** and **P2** in dilute DCB solutions and as thin films are shown in Figure 2. In solutions both **P1** and **P2** exhibit a broad absorption with two peaks in the visible region. The absorption peaks are located at 431 and 614 nm for **P1** and 421 and 591 nm for **P2**. Compared with their solution absorption spectra, the corresponding film ones were red-shifted due to the aggregation of polymer chains in the solid state. All the solution and film optical absorption data are summarized in Table 2. The film absorption onsets (λ_{edge}) of **P1** and **P2** are 747 and 729 nm, respectively. The optical band gaps ($E_{g,opt}$) of **P1** and **P2** were therefore calculated to be 1.66 and 1.70 eV, respectively, according to the equation: $E_{g,opt}$ = 1240/absorption onset.

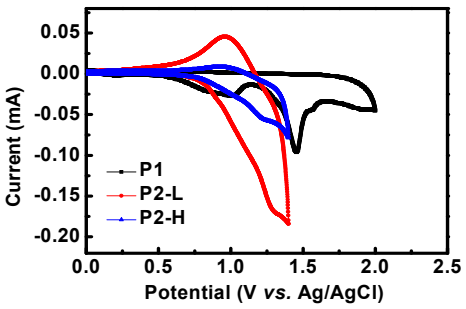

Fig. 3 Cyclic voltammograms of P1, P2-L, and P2-H in films on a platinum electrode in 0.1 mol/L Bu_4NPF_6 acetonitrile solution at a scan rate of 100 mV/s

Transport Properties. Hole mobility up to 10^{-3} $cm^2V^{-1}s^{-1}$ is usually required for polymer donors in order to obtain balanced electron and hole mobility for the polymer and PCBM blends, and balanced mobility is very crucial for achieving high performance polymer solar cells. Transport properties of polymers were therefore investigated by fabrication of field effect transistors (FETs). Bottom-contact devices were fabricated on Si/SiO_2 substrates with the low resistance Si as channel width, L is the channel length, C_i is the capacitance per unit area of the gate dielectric layer (SiO_2, 500 nm, C_i = 11 nF/cm^2), and V_G and V_T is the gain voltage and threshold voltage, respectively. Hole mobilities, V_T, and on/off ratios are summarized in Table 3, the detailed data are shown in Table S1. Transfer characteristic and output characteristic of polymers are shown in Figure S1. Hole mobilities of these polymers are close to the electron mobility of $PC_{71}BM$.

Table 3. FET properties of the pure polymer films

polymers	Annealing temperature	on/off	μ (cm^2/Vs)	V_T (V)
P1	200 °C	1.07±0.17×10^5	3.56±0.87×10^{-3}	-1.5±0.7
P2-L	200 °C	1.47±0.20×10^6	4.31±0.12×10^{-3}	-22.8±0.9
P2-H	250 °C	9.29±0.71×10^6	1.45±0.09×10^{-2}	-8.4±0.9

Journal Name RSCPublishing

ARTICLE

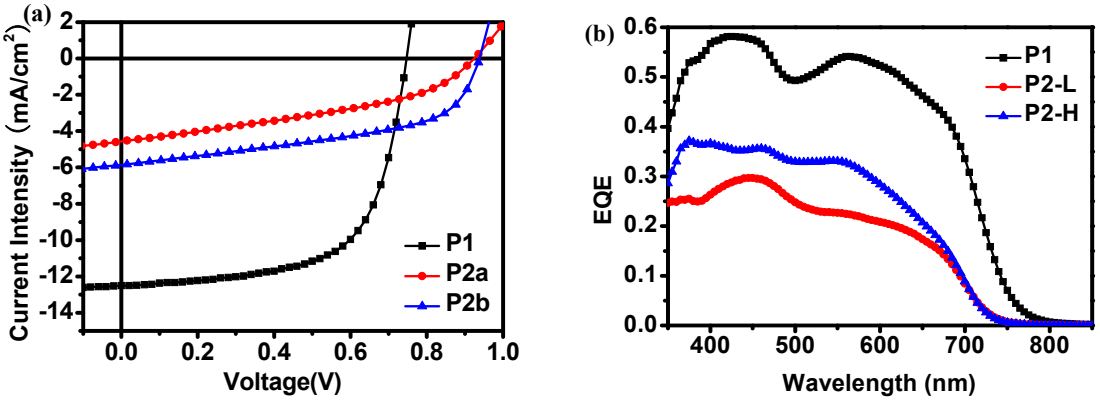

Fig. 4 (a) *J-V* curves of P1, P2-L, and P2-H solar cells; (b) External Quantum Efficiency curves for the solar cells devices with the best conditions

Table 4. Photovoltaic properties of **P1**, **P2-L**, and **P2-H**

Polymer	V_{oc} (V)	J_{sc} (mA/cm^2)	FF	PCE (%)	Thickness (nm)
P1	0.74±0.01	12.18±0.47	0.63±0.03	5.7±0.3	112±10
P2-L	0.93±0.01	3.91±0.65	0.42±0.03	1.5±0.2	104±10
P2-H	0.94±0.01	5.41±0.49	0.46±0.04	2.5±0.2	106±10

Photovoltaic Properties. Photovoltaic properties of polymers were evaluated by using the device configuration of ITO/ZnO/active layer/MoO_3/Ag. The performance of devices was optimized by variation of the weight ratio of polymer to $PC_{71}BM$, the concentration of blend solution, and the spin-coating speed. *J-V* curves of PSCs based on these three polymers are illustrated in Figure 4(a). For **P1**, devices fabricated with the blends of **P1** and $PC_{71}BM$ in a weight ratio of 1:1.5 in DCB solutions gave the best device performance with a PCE of 6.0%, a V_{oc} of 0.74 V, a J_{sc} of 12.50 mA/cm^2, and an *FF* of 0.65. Devices fabricated with the blends of **P2-L** and $PC_{71}BM$ in a weight ratio of 1:1.5 in DCB solutions gave the best device performance with a PCE of 1.7%, a V_{oc} of 0.93 V, a J_{sc} of 4.54 mA/cm^2, and an *FF* of 0.40. For **P2-H**, a PCE of 2.8% with a V_{oc} of 0.94 V, a J_{sc} of 5.90 mA/cm^2, and an *FF* of 0.50 can be achieved with device fabricated under the same conditions like **P2-L**, and the data are summarized in Table 4. Ten devices were fabricated to give the average value of PCEs, the detailed results are shown in Table S2. The use of 1,8-diiodooctance (DIO) as the solvent additive for the processing of the active layer has been tried, but the photovoltaic performances are inferior to DIO free ones.

As shown in Figure 4(b), external quantum efficiencies (EQEs) were measured to examine the accuracy of J_{sc}, the devices was fabricated from the best conditions for each polymers. For **P1**, EQE value approached 0.6, leading to a high short circuit current for the devices. In comparison with **P1** based devices, **P2** based PSCs exhibited lower EQEs. The EQE value of **P2-H** based devices is higher than that of **P2-L** based devices. As observed for many conjugated polymers, high molecular weight materials usually gave high hole mobility and efficiency.

Film Morphology. Usually, the extension of lateral conjugation of conjugated polymers can give higher photovoltaic performance;[19] therefore, **P2** with two thienyl substituents on the benzodithiophene unit was anticipated to afford high PCE. To understand why **P1**:$PC_{71}BM$ based PSCs

Journal Name RSCPublishing

ARTICLE

gave much higher PCE than **P2**:$PC_{71}BM$ based PSCs. Nanostructures of blend films were therefore investigated by transmission electron microscopy (TEM), and the TEM images are shown in Figure 5. TEM investigations revealed that **P1**:$PC_{71}BM$ blend films are homogenous with nanoscale phase separation; whereas **P2-L**:$PC_{71}BM$ and **P2-H**:$PC_{71}BM$ blend films are of apparent phase separation with the domain size approximate to 100 nm. The large domains are probably formed by the aggregation of $PC_{71}BM$, indicating the poor miscibility between **P2** and $PC_{71}BM$. The formation of large isolated spherical aggregation of $PC_{71}BM$ is detrimental to the transportation of electron to the collecting electrode.

Conclusions

We have designed and synthesized two conjugated polymers based on difluoro-substituted dibenzo[a,c]phenazine and benzodithiophene derivations. The as-synthesized two polymers were carefully characterized and used as the donor material in the BHJ PSCs. **P1** gave the best device performance with PCE of 6.0%, a V_{oc} of 0.74 V, and a J_{sc} of 12.50 mA/cm^2. Both the main chain and side chain play important roles to the performance of polymer solar cells. The optical property is mainly determined by the main chain structures; whereas the side chains can significantly influence the morphology of blend films. If the polymers have similar optical properties, their photovoltaic performance can be enhanced by optimizing the morphology of blend films through changing different side chains. Influences of side chains and the molecular weight on the photovoltaic performance of PSCs were also investigated. Compared to **P1**, **P2-H** with two lateral 2,3-didecylthiophene on the benzodithiophene unit has high molecular weight and better solubility in commonly used organic solvents. The formation of large aggregations in the **P2**-H:$PC_{71}BM$ blend films made the photovoltaic performance of **P2-H** inferior to that of **P1**.

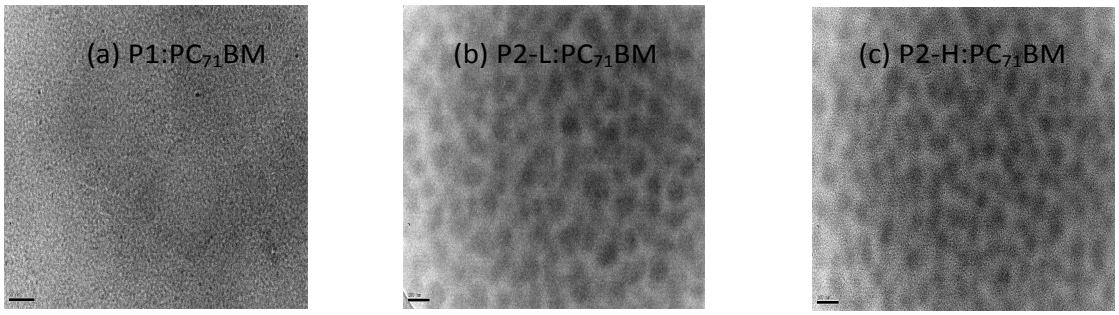

Fig.5 TEM images of P1:$PC_{71}BM$, P2-L:$PC_{71}BM$ and P2-H:$PC_{71}BM$ blend films in a weight ratio of polymer to $PC_{71}BM$ of 1:1.5. The scale bar is 100 nm

Acknowledgements

We express thanks for the financial support by the NSF of China (51003006 and 21161160443), the 973 Programs (2011CB935702), and the Fundamental Research Funds for the Central Universities.

Notes and references

[1]Beijing Key Laboratory of Energy Conversion and Storage Materials, College of Chemistry, Beijing Normal University, Beijing 100875, China
E-mail: zsbo@bnu.edu.cn; licuihong@bnu.edu.cn

†Electronic Supplementary Information (ESI) available: [^{1}H and ^{13}C NMR spectra, experimental part including detailed mobility results and solar cells results]. See DOI: 10.1039/b000000x/

1. S. Günes, H. Neugebauer and N. S. Sariciftci, *Chem. Rev.*, 2007, **107**, 1324-1338.
2. F. C. Krebs, *Sol. Energ. Mater. Sol. C.*, 2009, **93**, 393.
3. G. Dennler, M. C. Scharber and C. J. Brabec, *Adv. Mater.*, 2009, **21**, 1323-1338.
4. Y. Li, *Acc. Chem. Res.*, 2012, **45**, 723-733.
5. Y.-J. Cheng, S.-H. Yang and C.-S. Hsu, *Chem. Rev.*, 2009, **109**, 5868-5923.
6. Y. Chen, X. Wan and G. Long, *Acc. Chem. Res.*, 2013, **46**, 2645-2655.
7. X. Guo, A. Facchetti and T. J. Marks, *Chem. Rev.*, 2014, ASAP.
8. J. Y. Kim, K. Lee, N. E. Coates, D. Moses, T.-Q. Nguyen, M. Dante and A. J. Heeger, *Science*, 2007, **317**, 222-225.
9. Z. He, C. Zhong, S. Su, M. Xu, H. Wu and Y. Cao, *Nat. Photon*, 2012, **6**, 591-595.
10. W. Li, A. Furlan, K. H. Hendriks, M. M. Wienk and R. A. J. Janssen, *J. Am. Chem. Soc.*, 2013, **135**, 5529-5532.
11. Q. Mei, C. Li, X. Gong, H. Lu, E. Jin, C. Du, Z. Lu, L. Jiang, X. Meng, C. Wang and Z. Bo, *ACS Appl. Mater. Interfaces*, 2013, **5**, 8076-8080.

12. J. J. Intemann, K. Yao, Y.-X. Li, H.-L. Yip, Y.-X. Xu, P.-W. Liang, C.-C. Chueh, F.-Z. Ding, X. Yang, X. Li, Y. Chen and A. K. Y. Jen, *Adv. Funct. Mater.*, 2014, **24**, 1465-1473.
13. Y.-J. Cheng, C.-H. Hsieh, Y. He, C.-S. Hsu and Y. Li, *J. Am. Chem. Soc.*, 2010, **132**, 17381-17383.
14. Z. He, C. Zhong, X. Huang, W.-Y. Wong, H. Wu, L. Chen, S. Su and Y. Cao, *Adv. Mater.*, 2011, **23**, 4636-4643.
15. C.-C. Chen, W.-H. Chang, K. Yoshimura, K. Ohya, J. You, J. Gao, Z. Hong and Y. Yang, *Adv. Mater.*, 2014, **26**, 5670-5677.
16. J. Chen and Y. Cao, *Acc. Chem. Res.*, 2009, **42**, 1709-1718.
17. Y. Liang and L. Yu, *Acc. Chem. Res.*, 2010, **43**, 1227-1236.
18. J. E. Coughlin, Z. B. Henson, G. C. Welch and G. C. Bazan, *Acc. Chem. Res.*, 2013, **47**, 257-270.
19. L. Ye, S. Zhang, L. Huo, M. Zhang and J. Hou, *Acc. Chem. Res.*, 2014, **47**, 1595-1603.
20. M. C. Scharber, D. Wuhlbacher, M. Koppe, P. Denk, C. Waldauf, A. J. Heeger and C. L. Brabec, *Adv. Mater.*, 2006, **18**, 789-794.
21. J.-H. Kim, C. E. Song, H. U. Kim, A. C. Grimsdale, S.-J. Moon, W. S. Shin, S. K. Choi and D.-H. Hwang, *Chem. Mater.*, 2013, **25**, 2722-2732.
22. E. Wang, L. Hou, Z. Wang, S. Hellström, F. Zhang, O. Inganäs and M. R. Andersson, *Adv. Mater.*, 2010, **22**, 5240-5244.
23. X. Guo, M. Zhang, J. Tan, S. Zhang, L. Huo, W. Hu, Y. Li and J. Hou, *Adv. Mater.*, 2012, **24**, 6536-6541.
24. H.-C. Chen, Y.-H. Chen, C.-C. Liu, Y.-C. Chien, S.-W. Chou and P.-T. Chou, *Chem. Mater.*, 2012, **24**, 4766-4772.
25. L. J. Lindgren, F. Zhang, M. Andersson, S. Barrau, S. Hellström, W. Mammo, E. Perzon, O. Inganäs and M. R. Andersson, *Chem. Mater.*, 2009, **21**, 3491-3502.
26. S. Hellström, P. Henriksson, R. Kroon, E. Wang and M. R. Andersson, *Org. Electron.*, 2011, **12**, 1406-1413.
27. H.-C. Chen, Y.-H. Chen, C.-H. Liu, Y.-H. Hsu, Y.-C. Chien, W.-T. Chuang, C.-Y. Cheng, C.-L. Liu, S.-W. Chou, S.-H. Tung and P.-T. Chou, *Polym. Chem.*, 2013, **4**, 3411-3418.
28. A. Iyer, J. Bjorgaard, T. Anderson and M. E. Köse, *Macromolecules*, 2012, **45**, 6380-6389.
29. T. Hu, L. Han, M. Xiao, X. Bao, T. Wang, M. Sun and R. Yang, *J. Mater. Chem. C*, 2014, **2**, 8047-8053.
30. Y. Zhang, J. Zou, H.-L. Yip, K.-S. Chen, D. F. Zeigler, Y. Sun and A. K. Y. Jen, *Chem. Mater.*, 2011, **23**, 2289-2291.
31. Y. Lee, Y. M. Nam and W. H. Jo, *J. Mater. Chem.*, 2011, **21**, 8583-8590.
32. H. J. Song, T. H. Lee, M. H. Han, J. Y. Lee and D. K. Moon, *Polymer*, 2013, **54**, 1072-1079.
33. J. Hai, W. Yu, E. Zhu, L. Bian, J. Zhang and W. Tang, *Thin Solid Films*, 2014, **562**, 75-83.
34. R. He, L. Yu, P. Cai, F. Peng, J. Xu, L. Ying, J. Chen, W. Yang and Y. Cao, *Macromolecules*, 2014, **47**, 2921-2928.
35. S. Li, Z. He, J. Yu, S. a. Chen, A. Zhong, R. Tang, H. Wu, J. Qin and Z. Li, *J. Mater. Chem.*, 2012, **22**, 12523-12531.
36. Y.-J. Cheng, C.-H. Chen, T.-Y. Lin and C.-S. Hsu, *Chem. Asian J.*, 2012, **7**, 818-825.
37. H. X. Zhou, L. Q. Yang, A. C. Stuart, S. C. Price, S. B. Liu and W. You, *Angew. Chem. Inter. Ed.*, 2011, **50**, 2995-2998.
38. H. J. Son, W. Wang, T. Xu, Y. Liang, Y. Wu, G. Li and L. Yu, *J. Am. Chem. Soc.*, 2011, **133**, 1885-1894.
39. S. C. Price, A. C. Stuart, L. Yang, H. Zhou and W. You, *J. Am. Chem. Soc.*, 2011, **133**, 4625-4631.
40. A. C. Stuart, J. R. Tumbleston, H. Zhou, W. Li, S. Liu, H. Ade and W. You, *J. Am. Chem. Soc.*, 2013, **135**, 1806–1815.
41. G. Li, C. Kang, X. Gong, J. Zhang, W. Li, C. Li, H. Dong, W. Hu and Z. Bo, *J. Mater. Chem. C*, 2014, 5116-5123.
42. R. P. Qin, W. W. Li, C. H. Li, C. Du, C. Veit, H. F. Schleiermacher, M. Andersson, Z. S. Bo, Z. P. Liu, O. Inganas, U. Wuerfel and F. L. Zhang, *J. Am. Chem. Soc.* 2009, **131**, 14612-14613.

